From Interstellar Clouds to Star-Forming Galaxies: Universal Processes?, E49, 1 of 2
Proceedings IAU Symposium No. 315, 2016
P. Jablonka, Ph. André, & F. van der Tak, eds.

doi:10.1017/S1743921316008103

Nature of highly extended CS(J=7-6) emission around low-mass protostar L483

Gigi Leung[1], **Jeremy Lim**[1] **and Shigehisa Takakuwa**[2]

[1]Department of Physics, University of Hong Kong,
Pok Fu Lam, Hong Kong
email: `jjlim@hku.hk`

[2]Academia Sinica Institute of Astronomy and Astrophysics,
P.O. Box23-141, Taipei 10617, Taiwan
email: `takakuwa@asiaa.sinica.edu.tw`

Abstract. Single-dish observations in CS(J=7-6) using the Atacama Submillimeter Telescope Experiment (ASTE) reveal emission extending out to thousands of AU from low-mass protostars, much larger than is expected based on simple models for their envelopes. Hypotheses for this emission invoke gas dispersed from the envelope surfaces facing the bipolar outflow cavities. Here, we combine interferometric data from the Submillimeter Array (SMA) with the previous single-dish data from ASTE for the low-mass protostar L483 to study the spatial-kinematic structure of its CS(J=7-6) emission on projected scales $\gtrsim$600 AU. In addition to providing more detailed information for the extended component, our combined maps reveal a compact central component in CS(J=7-6) having a steeper velocity gradient. Both the compact and extended components exhibit a velocity gradient in the opposite sense to that of a bipolar molecular outflow traced in CO(J=2-1). Finding that previous models make a number of wrong predictions for the observed features, we propose that both CS(J=7-6) components are produced by rotating and infalling gas along the envelope surfaces exposed by the bipolar outflow and therefore subjected to stellar irradiation and outflow compression.

Keywords. Stars: formation, molecular data, submillimeter

---

1. Results

CO(J=2-1): Figure 1 shows, in grey contours, the position-velocity (PV-) diagram of ^{13}CO(2-1) along (upper row) and across (lower row) the outflow axis, made from SMA data. Other than tracing a bipolar outflow elongated along east (redshifted)–west (blueshifted), the CO(J=2-1) emission exhibit a kinematically distinct compact central component confined to within ~1000 AU (1 arcsecond corresponds to a distance of 200 AU) from the protostar. This compact central component exhibits a velocity gradient in the opposite sense to the bipolar outflow. Furthermore, unlike the bipolar outflow, The compact central component also exhibits a velocity gradient across the outflow axis.

CS(J=7-6): The CS(7-6) emission is elongated along the outflow axis, reaching up to 4000 AU from the protostar. Figure 1 shows the PV-diagram of CS in black contours. The CS emission can be kinematically separated into an extended and a compact central component, both having a velocity gradient in the opposite sense to the outflow. In addition, both components show a velocity gradient across the outflow axis. The radial velocity of the extended component increases inwards along the outflow axis. The compact central component exhibits a steeper velocity gradient along the outflow axis and reaches a higher line-of-sight velocity ($V_{\rm LOS}$). The CS and CO compact central component have similar spatial and kinematic structures.

2. Interpretation

A schematic diagram of our model is shown in Figure 1(*d*). The CS(7-6) emission comes from the envelope surfaces defining the outflow cavity that is irradiated by the protostar and

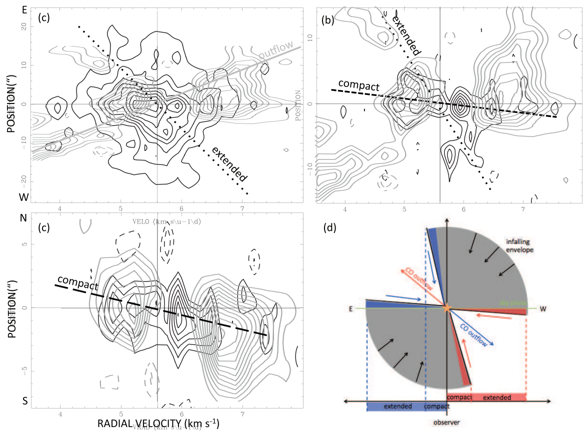

Figure 1. PV diagrams for CS(7-6) (black contours) and ^{13}CO(2-1) (grey contours) for a cut (*a*)&(*b*) along and (*c*) across the outflow axis. The PV-diagrams for CS(7-6) were made with (*a*): ASTE+SMA, dominated by the extended component; (*b*)&(*c*): SMA, dominated by the compact central component. The velocity gradients of the outflow, extended CS and compact CS & CO components are marked with solid, dotted and dashed lines respectively. Contours start at $2\,\sigma$. Black contours are plotted in steps of $2\,\sigma$ for (*a*)&(*c*), and $1\,\sigma$ for (*b*) (σ=0.5 Jy beam^{-1}). Grey contours are plotted in steps of $1\,\sigma$ (σ=0.3 Jy beam^{-1}). In each panel, the horizontal line indicates the position of the protostar, and the vertical line the systemic velocity. The schematic diagram of the infalling and rotating envelope model is shown in (*d*). The CS emitting region are marked with blue (blueshifted) and red (redshifted) triangular slabs.

compressed by the outflow. The inferred half-opening angle of the outflow cavity of L483 is 35° (Velusamy *et al.* 2014) and the inclination of the outflow axis is ∼40° from the sky plane (Fuller *et al.* 1995). With such a geometry, only infall can give rise to a velocity gradient in an opposite sense to the bipolar outflow. In addition, rotation of the envelope gives rise to the velocity gradients across the outflow axis. The extended CS component come from the infalling surfaces that lie closer to the sky plane. The inward increase of radial velocity is consistent with infall onto a central mass. The compact central component comes from the infalling surfaces that lie closer to the line of sight and therefore has a steeper velocity gradient and reaches a higher $V_{\rm LOS}$.

References

Fuller, G. A., Lada, E. A., Masson, C. R., & Myers, P. C. 1995, *ApJ*, 453, 754

Velusamy, T., Langer, W. D., & Thompson, T. 2014, *ApJ*, 783, 6

https://doi.org/10.1017/S1743921316008103 Published online by Cambridge University Press